Solutions of Schrödinger equation and thermal properties of generalized trigonometric Pöschl-Teller potential

C.O. Edet[a], P.O. Amadi[a], U.S. Okorie[a,b], A. Taş[c], A.N. Ikot[d,a] and G. Rampho[d]
[a]*Department of Physics, Theoretical Physics Group, University of Port Harcourt, Choba, Nigeria.*
e-mail: collinsokonedet@gmail.com
[b]*Department of Physics, Akwa Ibom State University, Ikot Akpaden, P.M.B. 1167, Uyo. Nigeria.*
[c]*Opticianry Programme, Health Services Vocational College, Harran University, Şanlıurfa, Turquey.*
[d]*Department of Physics, University of South Africa, South Africa.*

Received 19 August 2020; accepted 30 August 2020

Analytical solutions of the Schrödinger equation for the generalized trigonometric Pöschl-Teller potential by using an appropriate approximation to the centrifugal term within the framework of the Functional Analysis Approach have been considered. Using the energy equation obtained, the partition function was calculated, and other relevant thermodynamic properties. More so, we use the concept of superstatistics to evaluate the thermodynamics properties of the system. It is noted that the well-known normal statistics results are recovered in the absence of the deformation parameter $(q = 0)$, and this is displayed graphically for the clarity of our results. We also obtain the normalized wave function in terms of the hypergeometric function. The numerical energy spectra for different values of the principal and orbital quantum numbers are obtained. To show the accuracy of our results, we discuss some special cases by adjusting some potential parameters and also compute the numerical eigenvalue of the trigonometric Pöschl-Teller potential for comparison sake. However, it was found out that our results agree excellently with the results obtained via other methods.

Keywords: Trigonometric Pöschl-Teller potential; factorization method; superstatistics; Schrödinger equation.

PACS: 03.65.pm; 03.65.Ge; 03.65.Db; 34.20.Cf; 05.20.-y

DOI: https://doi.org/10.31349/RevMexFis.66.824

1. Introduction

The solutions of the radial Schrödinger equation is of immense importance in nonrelativistic quantum mechanics because it is well established that the wave function contains all the necessary information required to describe a quantum system [1-3]. From the early days of quantum mechanics, the study of exactly solvable problems has attracted considerable attention in many branches of physics. In particular, the applications of quantum mechanics to nuclear physics, information theory, molecular physics, and particle physics need not be overemphasized [4,5].

It is well known that exact solutions of this equation are only possible for a few potential models, such as the Kratzer [6-7], Eckart potential [8-10], shifted Deng-Fan [11-14], Molecular Tietz potential [15-18], etc. The exact analytical solutions of the Schrödinger equation with some of these potentials are only possible for $\ell = 0$. For $\ell \neq 0$ states, one has to employ some approximations, such as the Pekeris approximation [17,18], to deal with the orbit centrifugal term or solve numerically [19,20]. Several mathematical approaches have been developed to solve differential equations arising from these considerations. They include the supersymmetric approach [21-24], Nikiforov-Uvarov method [25-27], asymptotic iteration method (AIM) [28-30], Feynman integral formalism [31-34], factorization formalism [35,36], Formula Method[37] exact quantization rule method [38-43], proper quantization rule[44-48], Wave Function Ansatz Method[49] etc...

The trigonometric Pöschl-Teller potential was proposed by Pöschl and Teller [50] in 1933, and it has been used in describing diatomic molecular vibration. This potential can be written as

$$V(r) = V_1 \cos ec^2(\alpha r) + V_2 \sec^2(\alpha r), \tag{1}$$

where parameters V_1 and V_2 describe the property of the potential well, whereas the parameter α is related to the range of this potential [51].

This potential has been applied to study diatomic molecular vibration. Ever since it was proposed in 1933, researchers have given much attention to the molecular potential. For example, Liu *et al.* [51] carried out a fermionic analysis with this potential. The bound state solutions have also been carried out in the relativistic regime by Falaye and Ikhdair [52], Chen [53], Candemir [54]. and Hamzavi [55].

Very recently, Hamzavi and Rajabi [56] also studied the s-wave solutions of the Schrödinger equation for this potential using the Nikiforov-Uvarov method. Hamzavi and Ikhdair [57] obtained the approximate solutions of the radial Schrödinger equation for the rotating trigonometric PT potential using the Nikiforov-Uvarov method. The energy eigenvalues and their corresponding eigenfunctions were calculated for arbitrary ℓ-states in closed form.

Motivated by Ref. [50-57], we propose a modification to the trigonometric Pöschl-Teller potential, called the Generalized trigonometric Pöschl-Teller potential. This potential is given as:

$$V(r) = V_1 \cos ec^2(\alpha r) + V_2 \sec^2(\alpha r) + V_3 \tan^2(\alpha r) + V_4 \cot^2(\alpha r), \quad (2)$$

where parameters V_1, V_2, V_3, and V_4 describe the property of the potential well, whereas the parameter α is related to the range of this potential. For what obtains in previous studies of the molecular potential, we modified the potential to allow for more physical application and comparative analysis to existing studies of the molecular potential. Besides, in molecular physics, it has also been established that potential energy functions with more parameters tend to fit experimental data than those with fewer parameters, and researchers have recently paid great attention to obtaining modified version of potential functions by employing dissociation energy and equilibrium bond length for molecular systems as explicit parameters. This model will be an important tool for spectroscopists to represent experimental data, verify measurements, and make predictions.

The first step in obtaining the thermodynamics properties of a given system is to calculate its vibrational partition function. The partition function, which explicitly depends on temperature, aids us to obtain other thermodynamics properties. The vibrational partition function for certain potential models can easily be obtained by calculating the rotation-vibrational energy levels of the system whose applications are widely used in statistical mechanics and molecular physics [58,59]. Different mathematical approaches have been employed by many researchers in evaluating partition functions, such as Poisson the summation formula [60], commulant expansion method [61], standard method [62], and Wigner-Kirkwood formulation [63]. Superstatistics is the topic of interest in statistical mechanics.

Superstatistics is a superposition of different statistics: One given by ordinary Boltzmann factor and another given by the fluctuation of the intensive parameter such as the inverse temperature. Superstatistics describe non-equilibrium systems with a stationary state and intensive parameter fluctuations and contains Tsallis statistics as a special case [64-72].

Therefore, it is the primary objective of the present work to study the Schrödinger equation for non-zero angular momentum with the generalized trigonometric Pöschl-Teller potential using the Functional Analysis Approach. We will also use the resulting energy equation to find the partition function, which will enable us to calculate other thermodynamics properties via statistical mechanics and superstatistics mechanics approach.

This paper is organized as follows. In Sec. 2, we derive the bound states of the Schrödinger equation with the generalized trigonometric PT potential using the FAA. In Sec. 3, we obtain the thermodynamic properties, which will be calculated using the expression for the partition function. In Sec. 4, we calculate the effective Boltzmann factor considering modified Dirac delta distribution in the deformed formalism. We obtain the statistical properties of the systems by using the superstatistics. In Sec. 5, we obtain the rotational-vibrational energy spectrum for some diatomic molecules with numerical results and discussion. In Sec. 6, we present special cases of the potential under consideration. Finally, in Sec. 7, we give a concluding remark.

2. Energy levels and wavefunctions

The radial part of the Schrödinger equation is given by [60];

$$\frac{d^2R_{n\ell}(r)}{dr^2}+\frac{2\mu}{\hbar^2}\left[E_{n\ell}-V(r)-\frac{\hbar^2\ell(\ell+1)}{2\mu r^2}\right]R_{n\ell}(r)=0. \quad (3)$$

Considering the generalized trigonometric Pöschl-Teller potential (Eq. (2)), we obtain the radial Schrödinger equation, Eq. (3) is rewritten as follows:

$$\frac{d^2R_{n\ell}(r)}{dr^2}+\frac{2\mu}{\hbar^2}\Bigg[E_{n\ell}-(V_1\cos ec^2(\alpha r)+V_2\sec^2(\alpha r) + V_3\tan^2(\alpha r)+V_4\cot^2(\alpha r)) - \frac{\hbar^2\ell(\ell+1)}{2\mu r^2}\Bigg]R_{n\ell}(r)=0. \quad (4)$$

This equation cannot be solved analytically for $\ell \neq 0$ due to the centrifugal term. Therefore, we must use an approximation to the centrifugal term. We use the following approximation [57]

$$\frac{1}{r^2} \cong \alpha^2\left[d_0+\frac{1}{\sin^2(\alpha r)}\right], \quad (5)$$

where $d_0 = 1/12$ is a dimensionless shifting parameter, and α is the screening parameter. It is noted that for a short-range potential, the relation Eq. (5) is a good approximation to $1/r^2$, as proposed by Greene and Aldrich [19,53] approximation. This implies that Eq. (5) is not a good approximation to the centrifugal barrier when the screening parameter becomes large. Thus, the approximation is valid when $\alpha r = 1$.

Inserting Eqs. (5) into Eq. (4), we have:

$$\frac{d^2R_{n\ell}(r)}{dr^2}+\frac{2\mu}{\hbar^2}\Bigg[E_{n\ell}-(V_1\cos ec^2(\alpha r)+V_2\sec^2(\alpha r) + V_3\tan^2(\alpha r)+V_4\cot^2(\alpha r)) - \frac{\hbar^2\ell(\ell+1)\alpha^2}{2\mu} \times\left(d_0+\frac{1}{\sin^2(\alpha r)}\right)\Bigg]R_{n\ell}(r)=0. \quad (6)$$

Using the coordinate transformation $\rho = \sin^2(\alpha r)$, Eq. (6) translates into,

$$4\rho(1-\rho)\frac{d^2R_{n\ell}(\rho)}{d\rho^2}+(2-4\rho)\frac{d^2R_{n\ell}(\rho)}{d\rho}+\frac{1}{\rho(1-\rho)} \times\big[-(\varepsilon+\eta_3+\eta_4-\gamma d_0)\rho^2+(\varepsilon+\eta_1-\eta_2 + 2\eta_4-\gamma d_0+\gamma)\rho-(\eta_1+\eta_4+\gamma)\big]R_{n\ell}(\rho)=0. \quad (7)$$

For Mathematical simplicity, let us introduce the following dimensionless notations:

$$\varepsilon = \frac{2\mu E_{n\ell}}{\hbar\alpha^2}, \quad \eta_i = \frac{2\mu V_i}{\hbar^2\alpha^2},$$
$$i = 1,2,3,4, \quad \gamma = \ell(\ell+1). \tag{8}$$

To solve Eq. (6), we propose the physical wave function as:

$$R_{n\ell}(\rho) = \rho^{\beta}(1-\rho)^{\delta} f(\rho), \tag{9}$$

where

$$\beta = \frac{1}{4} + \sqrt{\frac{1}{16} + \frac{(\eta_1+\eta_4+\gamma)}{4}} \tag{10}$$

and

$$\delta = \frac{1}{4} + \sqrt{\frac{1}{16} + \frac{(\eta_3+\eta_2)}{4}}. \tag{11}$$

On substitution of Eq. (9) into Eq. (7) leads to the following hypergeometric equation:

$$\rho(1-\rho)f''(\rho) + \left[\left(2\beta+\frac{1}{2}\right) - (2\beta+2\delta+1)\rho\right] f'(\rho)$$
$$- \left[(\beta+\delta)^2 - \frac{(\varepsilon+\eta_3+\eta_4-\gamma d_0)}{4}\right] f(\rho) = 0 \tag{12}$$

whose solutions are the hypergeometric functions

$$f(\rho) = {}_2F_1(a,b;c;\rho), \tag{13}$$

where

$$a = (\beta+\delta) - \frac{\sqrt{\varepsilon+\eta_3+\eta_4-\gamma d_0}}{2},$$
$$b = (\beta+\delta) + \frac{\sqrt{\varepsilon+\eta_3+\eta_4-\gamma d_0}}{2},$$
$$c = 2\beta + \frac{1}{2}. \tag{14}$$

By considering the finiteness of the solutions, the quantum condition is given by

$$(\beta+\delta) - \frac{\sqrt{\varepsilon+\eta_3+\eta_4-\gamma d_0}}{2} = -n \quad n = 0,1,2... \tag{15}$$

from which we obtain, the energy expression as

$$\varepsilon = \gamma d_0 - \eta_3 - \eta_4 + \frac{1}{4}\left[4n+2+\sqrt{1+4(\eta_3+\eta_2)}\right.$$
$$\left. + \sqrt{1+4(\eta_1+\eta_4+\gamma)}\right]^2. \tag{16}$$

Thus, if one substitutes the value of the dimensionless parameters in Eq. (8) into Eq. (16), we obtain the energy eigenvalues as:

$$E_{n\ell} = \frac{\hbar^2\alpha^2\ell(\ell+1)d_0}{2\mu} - V_3 - V_4\frac{\hbar^2\alpha^2}{8\mu}$$
$$\times \left[4n+2+\sqrt{1+\frac{8\mu V_3}{\hbar^2\alpha^2}+\frac{8\mu V_2}{\hbar^2\alpha^2}}\right.$$
$$\left. + \sqrt{\frac{8\mu V_1}{\hbar^2\alpha^2}+\frac{8\mu V_4}{\hbar^2\alpha^2}+(2\ell+1)^2}\right]^2. \tag{17}$$

The corresponding unnormalized wave function is obtained as

$$R_{n\ell}(\rho) = N_{n\ell}\rho^{\beta}(1-\rho)^{\delta}{}_2F_1$$
$$\times \left(-n, n+2(\beta+\delta), 2\beta+\frac{1}{2}, \rho\right), \tag{18}$$

where $N_{n\ell}$ is the normalization constant. $N_{n\ell}$ can be calculated by the normalization conditions of the wave function:

$$\int_0^{\infty} |R_{n\ell}(r)|^2 dr = 1, \tag{19}$$

Putting Eq. (18) into the Eq. (19) yields

$$\frac{|N_{n\ell}(r)|^2}{\alpha} I_n = 1, \tag{20}$$

where

$$I_n = \int_0^1 \rho^{2\beta-(1/2)}(1-\rho)^{2\delta-(1/2)}$$
$$\times \left[{}_2F_1(-n, n+2\beta+2\delta, \frac{1}{2}+2\beta, \rho)\right]^2 d\rho. \tag{21}$$

The integral I_n is calculated for different n values using the Mathematica software program for $\mathrm{Re}[\beta] > -(1/4)$ and $\mathrm{Re}[\delta] > -(1/4)$ as follows:

$$n = 0 \;\Rightarrow\; I_0 = \frac{\Gamma\left(\frac{1}{2}+2\beta\right)\Gamma\left(\frac{1}{2}+2\delta\right)}{2(\beta+\delta)\Gamma(2\beta+2\delta)},$$
$$n = 1 \;\Rightarrow\; I_1 = \frac{2\Gamma\left(\frac{3}{2}+2\beta\right)\Gamma\left(\frac{3}{2}+2\delta\right)}{(1+4\beta)^2(\beta+\delta+1)\Gamma(2\beta+2\delta+1)},$$

$$n=2 \;\Rightarrow\; I_2=\frac{16\Gamma\left(\frac{5}{2}+2\beta\right)\Gamma\left(\frac{5}{2}+2\delta\right)}{(1+4\beta)^2(3+4\beta)^2(\beta+\delta+2)\Gamma(2\beta+2\delta+2)},$$

$$n=3 \;\Rightarrow\; I_3=\frac{192\Gamma\left(\frac{7}{2}+2\beta\right)\Gamma\left(\frac{7}{2}+2\delta\right)}{(1+4\beta)^2(3+4\beta)^2(5+4\beta)^2(\beta+\delta+3)\Gamma(2\beta+2\delta+3)},$$

$$\vdots \qquad\qquad \vdots$$

$$n=m \;\Rightarrow\; I_m=\frac{m!2^{4m-1}\Gamma\left(m+\frac{1}{2}+2\beta\right)\Gamma\left(m+\frac{7}{2}+2\delta\right)[\Gamma(m+2\beta)\Gamma(4\beta)]^2}{(\beta+\delta+m)\Gamma(2\beta+2\delta+m)[\Gamma(2\beta)\Gamma(2m+4\beta)]^2}, \tag{22}$$

Hence, we find

$$N_{nl}=\left(\frac{\alpha(\beta+\delta+n)\Gamma(2\beta+2\delta+n)[\Gamma(2\beta)\Gamma(2n+4\beta)]^2}{n!2^{4n-1}\Gamma\left(n+\frac{1}{2}+2\beta\right)\Gamma\left(n+\frac{7}{2}+2\delta\right)[\Gamma(n+2\beta)\Gamma(4\beta)]^2}\right)^{1/2}. \tag{23}$$

By using Eqs. (23) and (18) one can plot the radial wave functions for arbitrary quantum states through the Mathematica software program.

3. Thermal Properties of generalized trigonometric Pöschl-Teller potential

We consider the contribution of the bound state to the vibrational partition function at a given temperature T [58,60]

$$Z(\beta)=\sum_{n=0}^{n_{\max}} e^{-\beta E_{n\ell}}, \quad \beta=\frac{1}{k_BT}. \tag{24}$$

Here, k_B is the Boltzmann constant, and $E_{n\ell}$ is the rotational-Vibrational energy of the nth bound state.

We can rewrite Eq. (17) to be of the form

$$E_{n\ell}=\sigma_1+\frac{\hbar^2\alpha^2}{8\mu}(4n+\sigma_2)^2, \tag{25}$$

where

$$\sigma_1=\frac{\hbar^2\alpha^2\ell(\ell+1)d_0}{2\mu}-V_3-V_4;$$

$$\sigma_2=2+\sqrt{1+\frac{8\mu V_3}{\hbar^2\alpha^2}+\frac{8\mu V_2}{\hbar^2\alpha^2}}+\sqrt{\frac{8\mu V_1}{\hbar^2\alpha^2}+\frac{8\mu V_4}{\hbar^2\alpha^2}+(2\ell+1)^2}. \tag{26}$$

We substitute Eq. (25) into Eq. (24) to have

$$Z(\beta)=\sum_{n=0}^{n_{\max}} e^{-\beta[\sigma_1+(\hbar^2\alpha^2/8\mu)(4n+\sigma_2)^2]} \tag{27}$$

where

$$n_{\max}=\left|\frac{\sigma_2}{4}\right|. \tag{28}$$

Replacing the sum in Eq.(27) by an integral in the classical limit, we obtain

$$Z(\beta)=\int_0^{n_{\max}} e^{-\beta(An^2+Bn+C)}dn, \tag{29}$$

where

$$A=\frac{2\hbar^2\alpha^2}{\mu}; \quad B=\frac{\hbar^2\alpha^2\sigma_2}{\mu}; \quad C=\frac{\hbar^2\alpha^2\sigma_2^2}{8\mu}. \tag{30}$$

Therefore, we use the mathematica software to evaluate the integral in Eq. (29), thus obtaining the partition function for generalized trigonometric Pöschl-Teller potential model.

$$Z(\beta)=\frac{\sqrt{\pi}e^{(\beta B^2/4A)}\left(Erf\left(\frac{\beta(2An_{\max}+B)}{2\sqrt{\beta A}}\right)-Erf\left(\frac{\beta B}{2\sqrt{\beta A}}\right)\right)e^{-\beta C}}{2\sqrt{\beta A}}. \tag{31}$$

The imaginary error function can be defined as [62]

$$erfi(z)=ierf(z)=\frac{2}{\sqrt{\pi}}\int_0^z e^{u^2}du. \tag{32}$$

Thermodynamic functions such as; free energy, entropy, internal energy, and specific heat capacity functions can be obtained from the partition function (31) as follows [20].

3.1. Helmholtz free energy

$$F(\beta) = -\frac{1}{\beta}\ln z(\beta), \tag{33a}$$

$$F(\beta) = \frac{\ln\left(\dfrac{e^{(\beta B^2/4A)-\beta C}\sqrt{\pi}\left(Erf\left(\frac{\beta(2An_{\max}+B)}{2\sqrt{\beta A}}\right) - Erf\left(\frac{\beta B}{2\sqrt{\beta A}}\right)\right)}{2\sqrt{\beta A}}\right)}{\beta} \tag{33b}$$

3.2. Entropy

$$S(\beta) = -k_B\frac{\partial F(\beta)}{\partial\beta}, \tag{34a}$$

$$S(\beta) = \Delta_0 - \frac{(\Delta_1+\Delta_2+\Delta_3)}{\left(2\left(-Erf\left[\frac{B\sqrt{B}}{2\sqrt{A}}\right] + Erf\left[\frac{\sqrt{\beta}(B+2An_{\max})}{2\sqrt{A}}\right]\right)\right)}, \tag{34b}$$

where

$$\Delta_0 = \ln\left(\frac{e^{(\beta B^2/4A)-\beta C}\sqrt{\pi}\left(Erf\left[\frac{\beta(2An_{\max}+B)}{2\sqrt{\beta A}}\right] - Erf\left[\frac{\beta B}{2\sqrt{\beta A}}\right]\right)}{2\sqrt{\beta A}}\right),$$

$$\Delta_1 = Erf\left[\frac{B\sqrt{\beta}}{2\sqrt{A}}\right] - Erf\left[\frac{\sqrt{\beta}(B+2An_{\max})}{2\sqrt{A}}\right],$$

$$\Delta_2 = 2\left(\frac{B^2}{4A}-C\right)\beta\left(-Erf\left[\frac{B\sqrt{\beta}}{2\sqrt{A}}\right] + Erf\left[\frac{\sqrt{\beta}(B+2An_{\max})}{2\sqrt{A}}\right]\right),$$

$$\Delta_3 = \frac{e^{-(\beta[B+2An_{\max}]^2)/2A}\sqrt{\beta}(B - Be^{\beta n_{\max}(B+An_{\max})} + 2An_{\max})}{\sqrt{A}\sqrt{\pi}}. \tag{34c}$$

3.3. Internal energy

$$U(\beta) = -\frac{\partial(\ln Z(\beta))}{\partial\beta}, \tag{35a}$$

$$U(\beta) = \frac{1}{8A^{3/2}\beta^{3/2}}e^{-\beta[C+n_{\max}(B+An_{\max})]}\left(e^{[\beta(B+2An_{\max})^2]/4A}\sqrt{\pi}(-B^2\beta + A(2+4C\beta))\right.$$
$$\left.\times\left(-Erf\left[\frac{B\sqrt{B}}{2\sqrt{A}}\right] + Erf\left[\frac{\sqrt{\beta}(B+2An_{\max})}{2\sqrt{A}}\right]\right)\right) - 2\sqrt{A}\sqrt{\beta}(B - Be^{\beta n_{\max}(B+An_{\max})} + 2An_{\max}) \tag{35b}$$

3.4. Specific heat capacity

$$C_v = k_\beta\frac{\partial U(\beta)}{\partial\beta}, \tag{36a}$$

$$C_v = \frac{1}{32A^{5/2}}e^{(B^2\beta/4A)-C\beta}\left(H_0 + 2\sqrt{A}e^{-[\beta(B+2An_{\max})^2]/4A}(H_1+H_2)\right), \tag{36b}$$

$$H_0 = \frac{\sqrt{\pi}(12A^2 + 4A(-B^2+4AC)\beta + (B^2-4AC)^2\beta^2)\left(Erf\left[\frac{B\sqrt{B}}{2\sqrt{A}}\right] - Erf\left[\frac{\sqrt{\beta}(B+2An_{\max})}{2\sqrt{A}}\right]\right)}{\sqrt{\beta}}, \tag{36c}$$

$$H_1 = Be^{\beta n_{\max}(B+An_{\max})}(B^2\beta - 2A(3+4C\beta)),$$

$$H_2 = (B+2An_{\max})(-B^2\beta + A(6+8C\beta) + 4A\beta n_{\max}(B+An_{\max})).$$

4. Superstatistics mechanics

In this section, we introduce the necessary conditions of superstatistics. The effective Boltzmann factor of the system can be written as [73,74]

$$B(E) = \int_0^\infty e^{-\beta' E} f(\beta', \beta) d\beta', \tag{37}$$

where

$$f(\beta', \beta) = \delta(\beta' - \beta), \tag{38a}$$

is the probability density. Besides we state here the modified form of Dirac delta function used in this study as [75]:

$$f(\beta', \beta) = a'\delta(\beta' - \beta) + b'\beta' \frac{\partial}{\partial \beta'}(\delta(\beta' - \beta)) + c'\beta'^2 \frac{\partial^2}{\partial \beta'^2}(\delta(\beta' - \beta)). \tag{38b}$$

Finally, we find the generalized Boltzmann factor as in Ref. [75]

$$B(E) = e^{-\beta E}\left(1 + \frac{q}{2}\beta^2 E^2\right). \tag{39}$$

where q is the deformation parameter. Details of Eq. (39) can be found in Appendix A of Ref. [75] and references therein.

The partition function for the modified Dirac delta distribution has the following form [75]:

$$Z_S = \int_0^\infty B(E) dn. \tag{40}$$

We substitute Eq. (25) into Eq. (40) to have

$$Z_S = \int_0^\infty e^{-\beta[\sigma_1 + (\hbar^2\alpha^2/8\mu)(4n+\sigma_2)^2]} \times \left(1 + \frac{q}{2}\beta^2\left(\sigma_1 + \frac{\hbar^2\alpha^2}{8\mu}(4n+\sigma_2)^2\right)^2\right) dn. \tag{41}$$

Therefore, we use Mathematica software to evaluate the integral in Eq. (41), thus obtaining the partition function with generalized trigonometric Pöschl-Tellerpotential model in superstatistics as follows:

$$Z_q(\beta) = \frac{e^{-\beta(\sigma_1 + \lambda\sigma_2^2)}\left(e^{\beta\lambda\sigma_2^2}\sqrt{\pi}(8 + 3q + 4q\beta\sigma_1(1 + \beta\sigma_1)) - \sqrt{\beta\lambda}(\xi)\sigma_2 + 4q(\beta\lambda)^{3/2}\sigma_3^2\right)}{64\sqrt{\beta\lambda}} \tag{42a}$$

where

$$\xi = -6q - 8q\beta\sigma_1 + \frac{e^{\beta\lambda\sigma_2^2}\sqrt{\pi}Erf[\sqrt{\beta}\sqrt{\lambda}\sigma_2]}{\sqrt{\beta}\sqrt{\lambda}\sigma_2}. \tag{42b}$$

Other thermodynamic functions such as Helmholtz free energy, $F_S(\beta)$, entropy, $S_S(\beta)$, internal energy, $U_S(\beta)$, and specific heat, $C_S(\beta)$, functions can be obtained from the partition function (42a) as follows:

4.1. Helmholtz free energy

The Helmholtz free energy is obtained in superstatistics formalism with the aid of Eq. (33a) as follows:

$$F_q(\beta) = \frac{1}{\beta}\ln\left[\left(\frac{1}{64\sqrt{\beta\lambda}}\right)e^{-\beta(\sigma_1 + \lambda\sigma_2^2)}\left(N_0 - \sqrt{\beta\lambda}(-6q - 8q\beta\sigma_1 + N_1)\sigma_2 + 4q(\beta\lambda)^{3/2}\sigma_3^2\right)\right] \tag{43a}$$

where

$$N_0 = e^{-\beta\lambda\sigma_2^2}\sqrt{\pi}(8 + 3q + 4q\beta\sigma_1(1 + \beta\sigma_1)),$$
$$N_1 = \frac{e^{-\beta\lambda\sigma_2^2}\sqrt{\pi}Erf[\sqrt{\beta}\sqrt{\lambda}\sigma_2](8 + 3q + 4q\beta\sigma_1(1 + \beta\sigma_1))}{\sqrt{\beta}\sqrt{\lambda}\sigma_2}. \tag{43b}$$

4.2. Entropy

The entropy is obtained in superstatistics formalism with the aid of Eq. (34a) as follows:

$$S_q(\beta) = \Omega_0 + \frac{\Omega_1 + \Omega_2 - \Omega_3 + \Omega_4}{(2(\Omega_5 + \Omega_6))} \tag{44a}$$

where

$$\Omega_0 = \ln\left[\frac{1}{64\sqrt{\beta\lambda}}e^{-\beta(\sigma_1+\lambda\sigma_2^2)}\Big(e^{\beta\lambda\sigma_2^2}\sqrt{\pi}(8+3q+4q\beta\sigma_1(1+\beta\sigma_1))-\sqrt{\beta\lambda}(-6q-8q\beta\sigma_1+N_1)\sigma_2+4q(\beta\lambda)^{3/2}\sigma_2^3\Big)\right],$$

$$\Omega_1 = e^{\beta\lambda\sigma_2^2}\sqrt{\pi}(8+3q)\left(\sqrt{\beta}\sqrt{\lambda}-\sqrt{\beta\lambda}Erf\left[\sqrt{\beta}\sqrt{\lambda}\sigma_2\right]\right)+8e^{\beta\lambda\sigma_2^2}\sqrt{\pi}q\beta^3\left(\sqrt{\beta}\sqrt{\lambda}-\sqrt{\beta\lambda}Erf\left[\sqrt{\beta}\sqrt{\lambda}\sigma_2\right]\right)\sigma_1^3,$$

$$\Omega_2 = 2(8+3q)\sqrt{\beta}\sqrt{\lambda}\sqrt{\beta\lambda}\sigma_2+4q\beta^{3/2}\lambda^{3/2}\sqrt{\beta\lambda}\sigma_2^3+8q\beta^{5/2}\lambda^{5/2}\sqrt{\beta\lambda}\sigma_2^5,$$

$$\Omega_3 = 4q\beta^2\sigma_1^2\left(e^{\beta\lambda\sigma_2^2}\sqrt{\pi}\left(\sqrt{\beta}\sqrt{\lambda}-\sqrt{\beta\lambda}Erf\left[\sqrt{\beta}\sqrt{\lambda}\sigma_2\right]\right)-6\sqrt{\beta}\sqrt{\lambda}\sqrt{\beta\lambda}\sigma_2\right),$$

$$\Omega_4 = 2\beta\sigma_1\left(e^{\beta\lambda\sigma_2^2}\sqrt{\pi}(8+q)\left(\sqrt{\beta}\sqrt{\lambda}-\sqrt{\beta\lambda}Erf\left[\sqrt{\beta}\sqrt{\lambda}\sigma_2\right]\right)-2q\sqrt{\beta}\sqrt{\lambda}\sqrt{\beta\lambda}\sigma_2+12q\beta^{3/2}\lambda^{3/2}\sqrt{\beta\lambda}\sigma_2^3\right),$$

$$\Omega_5 = e^{\beta\lambda\sigma_2^2}\sqrt{\pi}(8+3q)\left(\sqrt{\beta}\sqrt{\lambda}-\sqrt{\beta\lambda}Erf\left[\sqrt{\beta}\sqrt{\lambda}\sigma_2\right]\right)+4e^{\beta\lambda\sigma_2^2}\sqrt{\pi}q\beta^2\left(\sqrt{\beta}\sqrt{\lambda}-\sqrt{\beta\lambda}Erf\left[\sqrt{\beta}\sqrt{\lambda}\sigma_2\right]\right)\sigma_1^2,$$

$$\Omega_6 = 6q\sqrt{\beta}\sqrt{\lambda}\sqrt{\beta\lambda}\sigma_2+4q\beta^{3/2}\lambda^{3/2}\sqrt{\beta\lambda}\sigma_2^3+4q\beta\sigma_1\Big(e^{\beta\lambda\sigma_2^2}\sqrt{\pi}\left(\sqrt{\beta}\sqrt{\lambda}-\sqrt{\beta\lambda}Erf\left[\sqrt{\beta}\sqrt{\lambda}\sigma_2\right]\right)$$
$$+2\sqrt{\beta}\sqrt{\lambda}\sqrt{\beta\lambda}\sigma_2\Big). \tag{44b}$$

4.3. Internal energy

The internal energy is obtained in superstatistics formalism with the aid of Eq. (35a) as follows:

$$U_q(\beta) = \frac{1}{128(\beta\lambda)^{3/2}}e^{-\beta(\sigma_1+\lambda\sigma_2^2)}\sqrt{\beta}\lambda^{3/2}\Big(e^{\beta\lambda\sigma_2^2}\sqrt{\pi}(8+3q)\left(\sqrt{\beta}\sqrt{\lambda}-\sqrt{\beta\lambda}Erf\left[\sqrt{\beta}\sqrt{\lambda}\sigma_2\right]\right)$$
$$+8e^{\beta\lambda\sigma_2^2}\sqrt{\pi}q\beta^3\left(\sqrt{\beta}\sqrt{\lambda}-\sqrt{\beta\lambda}Erf\left[\sqrt{\beta}\sqrt{\lambda}\sigma_2\right]\right)\sigma_1^3-4q\beta^2\sigma_1^2\Big(e^{\beta\lambda\sigma_2^2}\sqrt{\pi}\Big(\sqrt{\beta}\sqrt{\lambda}-\sqrt{\beta\lambda}Erf\left[\sqrt{\beta}\sqrt{\lambda}\sigma_2\right]\Big)$$
$$-6\sqrt{\beta}\sqrt{\lambda}\sqrt{\beta\lambda}\sigma_2\Big)2\sqrt{\beta}\sqrt{\lambda}\sqrt{\beta\lambda}\sigma_2\big(8+3q+2q\beta\lambda\sigma_2^2(1+2\beta\lambda\sigma_2^2)\big)$$
$$+2\beta\sigma_1\Big(e^{\beta\lambda\sigma_2^2}\sqrt{\pi}(8+q)\Big(\sqrt{\beta}\sqrt{\lambda}-\sqrt{\beta\lambda}Erf\left[\sqrt{\beta}\sqrt{\lambda}\sigma_2\right]\Big)+2q\sqrt{\beta}\sqrt{\lambda}\sqrt{\beta\lambda}\sigma_2(1+6\beta\lambda\sigma_2^2)\Big)\Big) \tag{45}$$

4.4. Specific heat capacity

The specific heat is obtained in superstatistics formalism with the aid of Eq. (36a) as follows:

$$C_q = \frac{1}{256(\beta\lambda)^{3/2}}e^{-\beta(\sigma_1+\lambda\sigma_2^2)}\sqrt{\beta}\sqrt{\lambda}\Big(\Xi_0-\Xi_1-6(8+3q)\sqrt{\beta}\sqrt{\lambda}\sqrt{\beta\lambda}\sigma_2-4(8+3q)\beta^{3/2}\lambda^{3/2}\sqrt{\beta\lambda}\sigma_2^3$$
$$+8q\beta^{5/2}\lambda^{5/2}\sqrt{\beta\lambda}\sigma_2^5-\Xi_2-\Xi_3-\Xi_4\Big), \tag{46a}$$

where

$$\Xi_0 = -3e^{\beta\lambda\sigma_2^2}\sqrt{\pi}(8+3q)\Big(\sqrt{\beta}\sqrt{\lambda}-\sqrt{\beta\lambda}Erf\Big[\sqrt{\beta}\sqrt{\lambda}\sigma_2\Big]\Big),$$

$$\Xi_1 = 16e^{\beta\lambda\sigma_2^2}\sqrt{\pi}q\beta^4\Big(\sqrt{\beta}\sqrt{\lambda}-\sqrt{\beta\lambda}Erf\Big[\sqrt{\beta}\sqrt{\lambda}\sigma_2\Big]\Big)\sigma_1^4,$$

$$\Xi_2 = 16q\beta^{7/2}\lambda^{7/2}\sqrt{\beta\lambda}\sigma_2^7+32q\beta^3\sigma_1^3\Big(e^{\beta\lambda\sigma_2^2}\sqrt{\pi}\Big(\sqrt{\beta}\sqrt{\lambda}-\sqrt{\beta\lambda}Erf\Big[\sqrt{\beta}\sqrt{\lambda}\sigma_2\Big]\Big)-2\sqrt{\beta}\sqrt{\lambda}\sqrt{\beta\lambda}\sigma_2\Big),$$

$$\Xi_3 = 8\beta^2\sigma_1^2\Big(e^{\beta\lambda\sigma_2^2}\sqrt{\pi}(4+q)\Big(\sqrt{\beta}\sqrt{\lambda}-\sqrt{\beta\lambda}Erf\Big[\sqrt{\beta}\sqrt{\lambda}\sigma_2\Big]\Big)-6q\sqrt{\beta}\sqrt{\lambda}\sqrt{\beta\lambda}\sigma_2+12q\beta^{3/2}\lambda^{3/2}\sqrt{\beta\lambda}\sigma_2^3\Big)$$

$$\Xi_4 = 8\beta\sigma_1\Big(e^{\beta\lambda\sigma_2^2}\sqrt{\pi}(4+q)\Big(\sqrt{\beta}\sqrt{\lambda}-\sqrt{\beta\lambda}Erf\Big[\sqrt{\beta}\sqrt{\lambda}\sigma_2\Big]\Big)+2(4+q)\sqrt{\beta}\sqrt{\lambda}\sqrt{\beta\lambda}\sigma_2$$
$$-4q\beta^{3/2}\lambda^{3/2}\sqrt{\beta\lambda}\sigma_2^3+8q\beta^{5/2}\lambda^{5/2}\sqrt{\beta\lambda}\sigma_2^5\Big). \tag{46b}$$

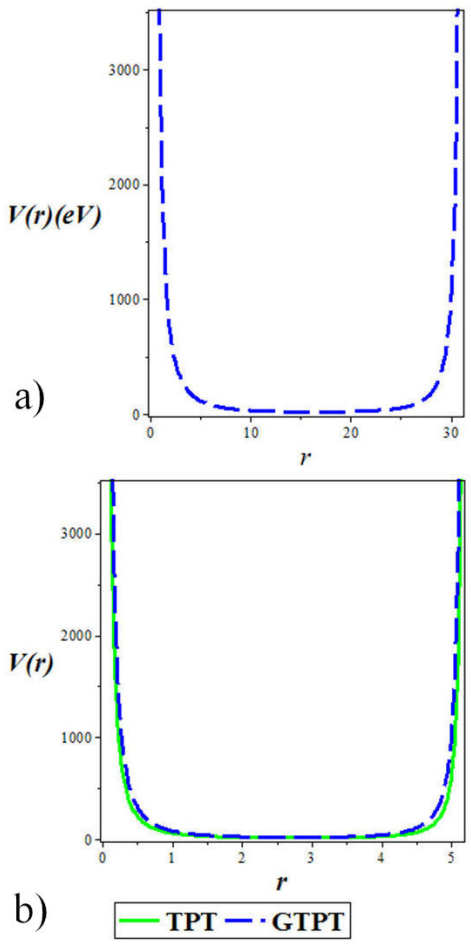

FIGURE 1. a) Shape of the generalized trigonometric Pöschl-Tellerpotential for different values of the screening parameter α. We chose $V_1 = 5\ fm^{-1}$, $V_2 = 3\ fm^{-1}$, $V_3 = 2\ fm^{-1}$, and $V_4 = 0.5\ fm^{-1}$. b) Shape of the trigonometric Pöschl-Tellerpotential model and generalized trigonometric Pöschl-Tellerpotential. We chose $V_1 = 5\ fm^{-1}$, $V_2 = 3\ fm^{-1}$, $V_3 = 2\ fm^{-1}$, $V_4 = 0.5\ fm^{-1}$, and $\alpha = 0.3$.

5. Numerical results and applications

To show the accuracy of our work, we calculate the energy eigenvalues using Eq. (18) for different quantum numbers n and ℓ with parameters $V_1 = 5\ fm^{-1}$, $V_2 = 3\ fm^{-1}$, $V_3 = 0.5$, $V_4 = 0.5$, and $\mu = 10\ fm^{-1}$. In Table I, it is observed that the energy decreases for a fixed value of the principal quantum number for varying orbital angular momentum. Furthermore, we have computed the energy eigenvalues of the trigonometric Pöschl-Teller potential using the reduced energy equation given in Eq. (33) and Eq.(34) as a special case. Our results, shown in Tables II- V,, are in good agreement with the results given in Ref. [56-57,76].

In Fig. 1a) and b), we plot the shape of the potential for clarity and understanding of the system we are studying. Figure 1a) we plot the shape of the generalized trigonometric Pöschl-Tellerpotential against the interatomic distance. Figure 1b) shows a comparative plot of the shapes of the trigonometric Pöschl-Tellerpotential model and generalized trigonometric Pöschl-Tellerpotential. However, we note that our generalized model fits appropriately with the trigonometric Pöschl-Tellerpotential.

Figures 2 a)-f) clearly shows the energy eigenvalues variation with parameters V_1, V_2, V_3, V_4, μ and α for various quantum states. It can be easily observed from these Figs. 2a)-d) that the parameters increase directly as the energy increases. Figure 2e) shows the energy eigenvalues variation with the particle's reduced mass μ for different quantum states. It is seen that in the region $\mu \approx 0 - 0.1\ a.m.u$, the energy eigenvalue is at its maximum, beyond this region, there is a drop and this continues in a linear trend. The energy is only high in the region where the mass is low but decreases as the particle's mass increases monotonically. The energy is very similar for $0.2 < \mu < 1.0$. Figure 2f) shows the energy eigenvalues variation with screening parameter α for different quantum states. It can be seen explicitly that in all the quantum states, the representation curves spreads out uniformly from the origin. It is shown that the energy eigenvalue increases as the screening parameter increases.

TABLE I. Bound state energy levels $E_{n\ell}$ for the Generalised trigonometric Pöschl-Teller potential obtained with parameters $V_1 = 5\ fm^{-1}$, $V_2 = 3\ fm^{-1}$, $V_3 = 0.5$, $V_4 = 0.5$, and $\mu = 10\ fm^{-1}$.

States	$\alpha = 0.002$	$\alpha = 0.02$	$\alpha = 0.2$	$\alpha = 0.4$	$\alpha = 0.8$	$\alpha = 1.2$
1s	18.50038334	18.61121709	19.73743352	21.0271324	23.72899708	26.59648864
2s	18.50858178	18.69348948	20.58899614	22.79449204	27.52159072	32.67406160
2p	18.50858258	18.69357133	20.59752395	22.83011829	27.67609429	33.04821322
3s	18.51678180	18.77592188	21.45655875	24.62585164	31.57018435	39.32763454
3p	18.51678262	18.77600388	21.46523908	24.66269723	31.73441612	39.73447216
3d	18.51678425	18.77616788	21.48259499	24.73630368	32.06125854	40.53875474
4s	18.52498345	18.85851426	22.34012135	26.52121126	35.87477799	46.55720749
4p	18.52498425	18.85859642	22.34895421	26.55927615	36.04873794	46.99673112
4d	18.52498588	18.85876072	22.36661499	26.63531596	36.39487055	47.86516178
4f	18.52498834	18.85900721	22.39309395	26.7491527	36.90974960	49.14313806

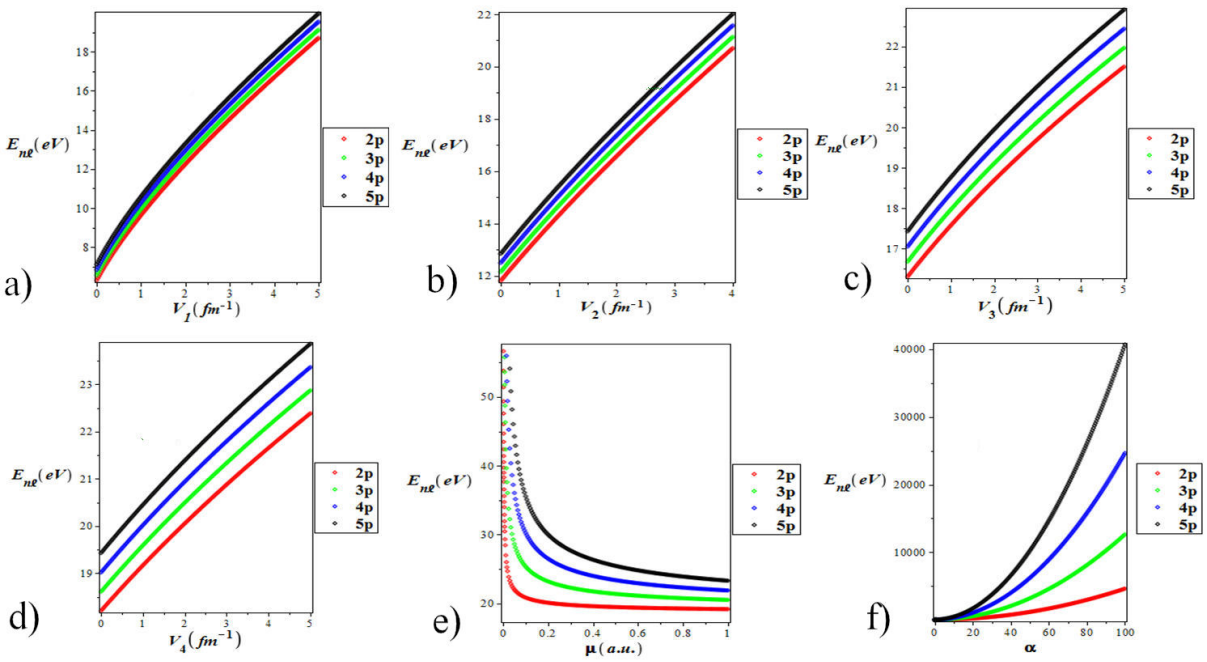

FIGURE 2. Energy eigenvalues variation with (a) parameter for various quantum states (b) parameter for various quantum states. (c) with parameter for various quantum states. (d) with parameter for various quantum states (e) with particle's mass for various quantum states. (f) with screening parameter for quantum states.

TABLE II. Comparison of s-wave energy eigenvalues (in eV) obtained by using the Functional Analysis Approachwith other methods for the trigonometric Pöschl-Teller potential with other methods obtained with parameters $V_1 = 5\ fm^{-1}$, $V_2 = 3\ fm^{-1}$, and $\mu = 10\ fm^{-1}$.

n	Present	AIM [64]	NU [56]	Present	AIM [64]	NU [56]	Present	AIM [64]	NU [56]
		$\alpha = 0.2$	$\alpha = 0.2$		$\alpha = 0.02$	$\alpha = 0.02$		$\alpha = 0.002$	$\alpha = 0.002$
0	16.10494172	16.104 941 73	16.104 941 72	15.78149898	15.781 498 98	15.781 498 98	15.7495163	15.749 516 29	15.749 516 29
1	16.83082621	16.830 826 21	16.830 826 21	15.8526429	15.852 642 89	15.852 642 89	15.75661628	15.756 616 28	15.756 616 28
2	17.5727107	17.572 710 70	17.572 710 70	15.9239468	15.923 946 80	15.923 946 80	15.76371788	15.763 717 86	15.763 717 86
3	18.33059519	18.330 595 18	18.330 595 18	15.99541072	15.995 410 71	15.995 410 71	15.77082105	15.770 821 05	15.770 821 05
4	19.10447968	19.104 479 67	19.104 479 67	16.06703462	16.067 034 63	16.067 034 63	15.77792584	15.777 925 84	15.777 925 84
5	19.89436415	19.894 364 16	19.894 364 16	16.13881855	16.138 818 54	16.138 818 54	15.78503222	15.785 032 22	15.785 032 22
6	20.70024864	20.700 248 64	20.700 248 64	16.21076245	16.210 762 45	16.210 762 45	15.79214021	15.792 140 21	15.792 140 21

TABLE III. Comparison of s-wave energy eigenvalues (in eV) obtained by using the Functional Analysis Approach with other methods for the trigonometric Pöschl-Teller potential with other methods obtained with parameters $V_1 = 5\ fm^{-1}$, $V_2 = 3\ fm^{-1}$, and $\mu = 10\ fm^{-1}$.

n	Present	NU [56]	Present	NU [56]	Present	NU [56]
		$\alpha = 1.2$		$\alpha = 0.8$		$\alpha = 0.4$
0	18.02560022	18.02560022	17.23163309	17.23163309	16.47211972	16.47211973
1	22.87051711	22.8705171	20.32991862	20.32991862	17.95616358	17.95616357
2	28.29143400	28.29143398	23.68420415	23.68420415	19.50420741	19.50420742
3	34.28835088	34.28835086	27.29448969	27.2944896	21.11625128	21.11625126
4	40.86126776	40.86126774	31.16077521	31.16077522	22.79229512	22.7922951
5	48.01018464	48.01018462	35.28306075	35.28306074	24.53233896	24.53233894
6	55.73510152	55.7351015	39.66134628	39.66134628	26.33638282	26.33638278

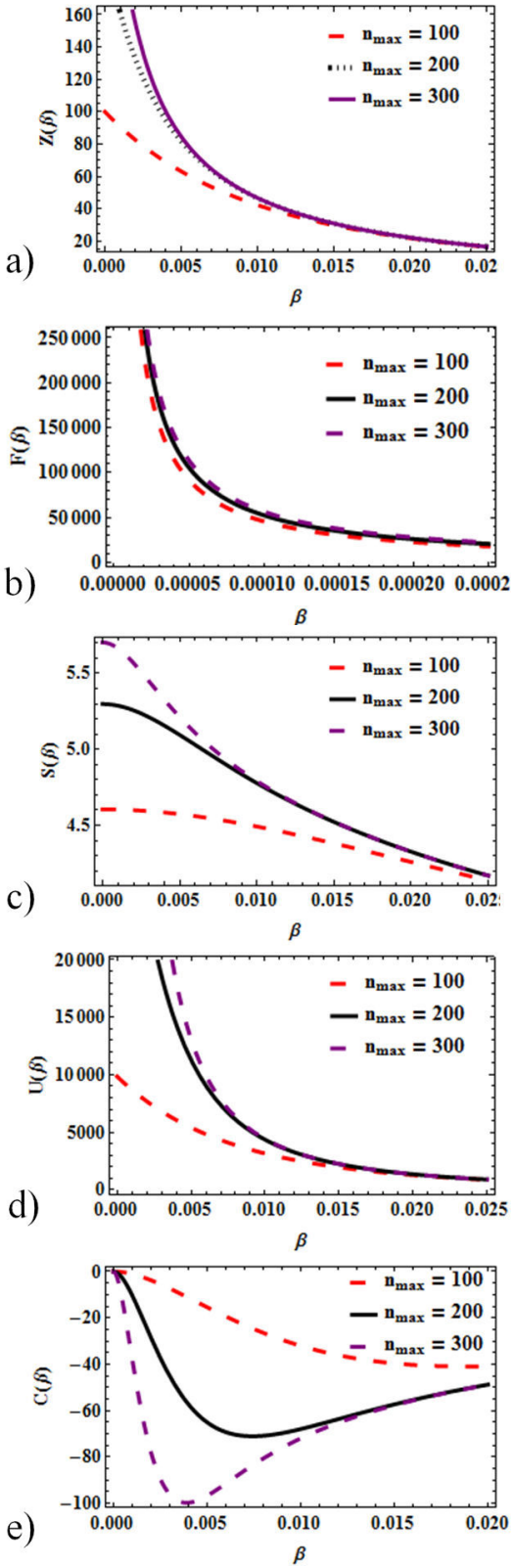

FIGURE 3. a) Partition Function variation with β for various values of $n_{\max}$. b) Free energy variation with for different values of $n_{\max}$. c) Entropy variation with β for different values of $n_{\max}$. d) Mean energy variation with β for different values of $n_{\max}$. e) specific heat capacity variation with β for different values of $n_{\max}$.

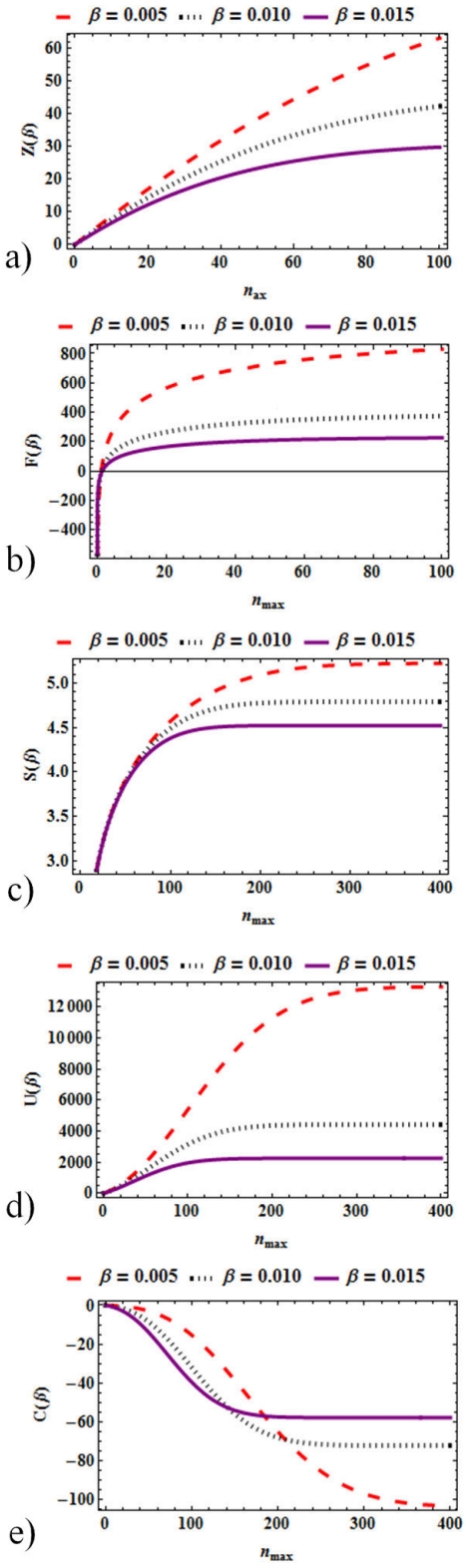

FIGURE 4. a) Partition Function variation with $n_{\max}$ for various values of β. b) Free energy variation with $n_{\max}$ for different values of β. c) Entropy variation with $n_{\max}$ for different values of β. d) Mean energy variation with $n_{\max}$ for different values of β. e) Specific heat capacity variation with $n_{\max}$ for different values of β.

In Figs. 3a)-e), we show a graphical representation of the thermal properties obtained via the standard Boltzmann-Gibbs statistical mechanical approach. We analyze how these properties vary with β for different discrete values of $n_{\max}$. Figure 3(a) shows the partition function variation with β for various values of $n_{\max}$. It can be seen that the partition function decreases as the temperature increases. It is also shown that in the high temperature limits, there's a uniform convergence of all the curves and the partition function reaches its minimum. Figure 3(b) shows the mean free energy variation with β for different values of $n_{\max}$. Again, it is seen that the free energy reduces monotonically with β. Figure 3(c) shows the entropy variation with β for different values of $n_{\max}$. It is seen that the entropy declines as temperature increases. Figure 3(d) shows the mean energy variation with β for various values of $n_{\max}$. The mean energy decreases as β increases. It is also observed that the mean energy has its minimum in the high β region. Figure 3(e) clearly shows the specific heat capacity variation with β for different values of $n_{\max}$. An asymmetric shaped formed for increasing value of $n_{\max}$. At $n_{\max} = 300$, its trough is reached and heat capacity monotonically growth with β. We see that at some point in β, the values of $n_{\max}$ might become invariant.

In Fig 4(a-e), we graphically display the thermal properties obtained via the standard Boltzmann-Gibbs statistical mechanical approach. We analyze how these properties vary with $n_{\max}$ for different values of β. Figure 4a) clearly shows the Partition Function variation with $n_{\max}$ for various values of β. From this plot, we observe that there is spread from the zero point; the partition function increases as $n_{\max}$ increases. It is also observed that the partition function has its maximum in the high region of $n_{\max}$. Figure 4b) clearly shows the free energy variation with $n_{\max}$ for different values of β. It is clearly shown that the mean free energy rises logarithmically as $n_{\max}$ rises. Figure 4c) shows a plot of entropy variation with different values of β. It is seen that the entropy up-

TABLE IV. Comparison of l-state energy eigenvalues (in eV) obtained by using the Functional Analysis Approach with other methods for the trigonometric Pöschl-Teller potential with other methods obtained with parameters $V_1 = 5\ fm^{-1}$, $V_2 = 3\ fm^{-1}$, and $\mu = 10\ fm^{-1}$.

States	Present	NU [57]	Present	NU [57]	Present	NU [57]	Present
		$\alpha = 1.2$		$\alpha = 0.8$		$\alpha = 0.4$	
1s	22.87051711	22.87051710	20.32991862	20.32991862	17.95616358	17.95616357	16.83082621
2s	28.29143400	28.29143398	23.68420415	23.68420415	19.50420741	19.50420742	17.57271070
2p	28.64395420	28.64395419	23.82847893	23.82847894	19.53712285	19.53712286	17.58054181
3s	34.28835088	34.28835086	27.29448969	27.2944896	21.11625128	21.11625126	18.33059519
3p	34.67512504	34.67512504	27.44896379	27.44896381	21.15044541	21.15044543	18.33858624
3d	35.43921159	35.43921159	27.75631555	27.75631556	21.21875332	21.2187533	18.35456400
4s	40.86126776	40.86126774	31.16077521	31.16077522	22.79229512	22.7922951	19.10447968
4p	41.28229588	41.28229584	31.32544867	31.32544868	22.82776799	22.8277680	19.11263069
4d	42.11348591	42.11348590	31.65300784	31.65300783	22.89862722	22.89862721	19.12892818
4f	43.33519178	43.33519178	32.14003976	32.14003977	23.00470172	23.00470171	19.15336296

TABLE V. Comparison of l-state energy eigenvalues (in eV) obtained by using the Functional Analysis Approach with other methods for the trigonometric Pöschl-Teller potential with other methods obtained with parameters $V_1 = 5\ fm^{-1}$, $V_2 = 3\ fm^{-1}$, and $\mu = 10\ fm^{-1}$.

States	Present	NU [57]	Present	NU [57]	Present	NU [57]
		$\alpha = 0.2$		$\alpha = 0.02$		$\alpha = 0.002$
1s	16.83082621	16.83082621	15.8526429	15.85264289	15.75661628	15.75661628
2s	17.5727107	17.5727107	15.9239468	15.9239468	15.76371788	15.76371786
2p	17.58054181	17.58054181	15.92402152	15.92402153	15.76371861	15.76371860
3s	18.33059519	18.33059518	15.99541072	15.99541071	15.77082105	15.77082105
3p	18.33858624	18.33858626	15.99548559	15.9954856	15.77082179	15.77082179
3d	18.35456400	18.35456399	15.99563535	15.99563534	15.77082329	15.77082328
4s	19.10447968	19.10447967	16.06703462	16.06703463	15.77792584	15.77792584
4p	19.11263069	19.1126307	16.06710967	16.06710967	15.77792658	15.77792658
4d	19.12892818	19.12892817	16.06725975	16.06725974	15.77792808	15.77792806
4f	19.15336296	19.15336297	16.06748486	16.06748485	15.77793030	15.77793030

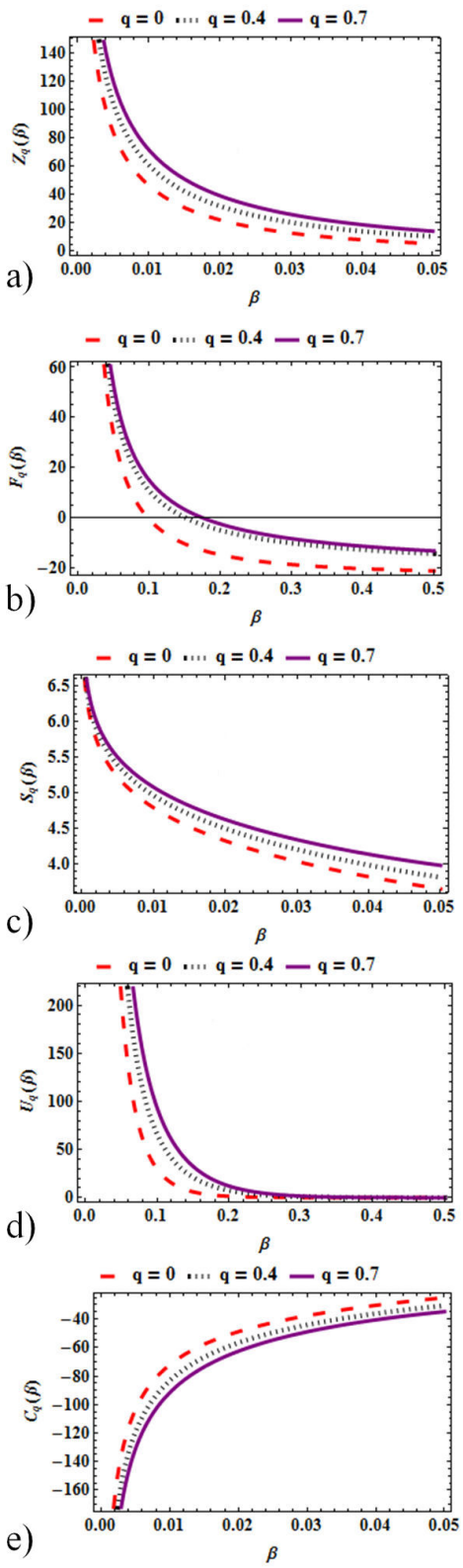

FIGURE 5. Superstatistics plots of: a) Partition Function variation with β for various values of q. b) Free energy variation with β for different values of q. c) Entropy variation with β for different values of q. d) Mean energy variation with β for different values of q. e) Specific heat capacity variation with β for different values of q.

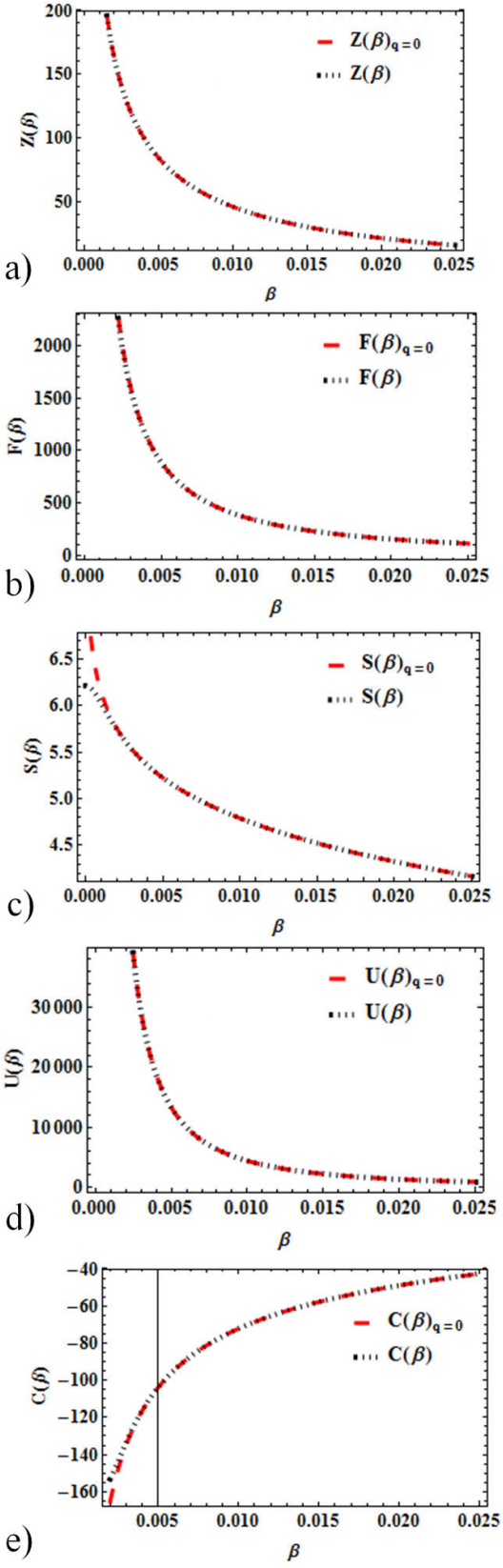

FIGURE 6. Comparison of superstatistics at $q = 0$ and normal statistics; a) Partition Function variation with β. b) Free energy variation with β. c) Entropy variation with β. d) Mean energy variation with β. e) Specific heat capacity variation with β.

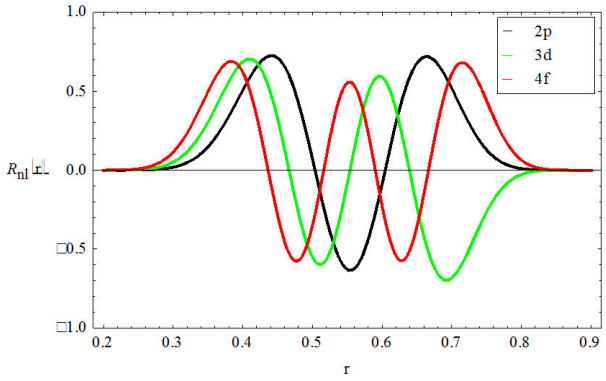

FIGURE 7. Variation of the bound states radial wave functions according to distance from nucleus r for different quantum states with $V_1 = 5\ fm^{-1}$, $V_2 = 3\ fm^{-1}$, $V_3 = 0.5\ fm^{-1}$, $V_4 = 0.5\ fm^{-1}$, $\alpha = 0.2$, and $\mu = 10\ fm^{-1}$.

surges monotonically with $n_{\max}$. Figure 4d) displays the plot of mean energy variation with $n_{\max}$ for different values of β. The mean energy surges in an linear-monotonic pattern. Figure 4e) presents the plot of specific heat capacity variation with $n_{\max}$ $n_{\max}$ for different values of β. As predicted in Fig. 3e), it clearly shows for the different values of β, at some point in $n_{\max}$, heat capacity becomes invariant. We can deduce that for the values of $n_{\max}$, specific heat and β is invariant.

In Fig 5(a-e), we show graphically the thermal properties obtained via the superstatistical mechanical approach. We analyze how these properties vary with β for different values of the deformation parameter q. Figure 5a) shows a plot of the partition function variation with β for various values of q. It is seen that the partition function decreases as β increases. More so, the partition function increases as q increases. Figure 5b) shows the variation of mean free energy with β for various values of q . The mean free energy decreases monotonically as β increases. A plot of entropy variation with β for different values of q is shown in Fig. 5c). The entropy of the system reduces as β rises. For different values of the deformation parameter, q, the entropy of the system increases with increasing q. Figure 5d) shows the variation of the mean energy with β for various values of q. The mean energy decreases with increasing β and increases with increasing q. Figure 5e) depicts a plot of specific heat capacity variation with β for different values of q. It is seen explicitly that the specific heat capacity of the system increases monotonically with increasing β but decreases with increasing q.

It is interesting to note also that when $q = 0$, normal statistics or the conventional Boltzmann-Gibbs statistics is recovered from the superstatistics. However, to further strengthen this claim. We show a graphical comparative plot in Figs. 6a)-e) of all thermal properties obtained via the superstatistics at $q = 0$ and B-G statistics at maximum quantum number. It is interesting to see that there's no discernable difference in the curves as they're both adequately fitted.

The shape of the radial wave functions is shown in Fig. 7 for $2p$, $3d$, and $4f$ quantum states. If we examine the shapes of Fig. 7 carefully, we see that the wave functions have different number of radial nodes and different amplitudes.

6. Special Cases

In this section, we shall study one special case of the Generalized Trigonometric Pöschl-Teller potential and its energy eigenvalues, respectively

6.1. Trigonometric Pöschl-Teller potential

Choosing $V_3 = V_4 = 0$, the Generalized Trigonometric Pöschl-Tellerpotential takes [76,56]

$$V(r) = \frac{V_1}{\sin^2(\alpha r)} + \frac{V_2}{\cos^2(\alpha r)}, \tag{47}$$

and the energy eigenvalue becomes

$$E_{n\ell} = \frac{\hbar^2\alpha^2\ell(\ell+1)d_0}{2\mu} + \frac{\hbar^2\alpha^2}{8\mu}\left[4n+2 + \sqrt{1+\frac{8\mu V_2}{\hbar^2\alpha^2}} + \sqrt{\frac{8\mu V_1}{\hbar^2\alpha^2}+(2\ell+1)^2}\right]^2. \tag{48}$$

This is in excellent agreement with Eq. (3) of Ref. [76] and Eq. (19) of Ref. [57].

By setting ℓ, we obtain the s-wave energy equation for the potential understudy as:

$$E_{n0}=\frac{\hbar^2\alpha^2}{8\mu}\left[4n+2+\sqrt{1+\frac{8\mu V_2}{\hbar^2\alpha^2}} + \sqrt{\frac{8\mu V_1}{\hbar^2\alpha^2}+1}\right]^2. \tag{49}$$

This is in excellent agreement with Eq. (15) of Ref. [56].

7. Conclusion

In this article, we have solved the Schrödinger equation using the Functional Analysis Approach and suitable approximation to overcome the centrifugal barrier. We have also presented the rotational-vibrational energy spectra with the Generalized Trigonometric Pöschl-Teller potential. We have expressed the solutions by the generalized hypergeometric functions ${}_2F_1(a,b,c\rho)$. Results have been discussed extensively using plots. We discussed some special cases by adjusting the potential parameters and compute the numerical energy spectra for the trigonometric Pöschl-Teller potential for both the $\ell = 0$ and $\ell \neq 0$ cases, respectively. It was found that our results agree with the existing literature. In detail, we evaluated the vibrational partition functions $Z(\beta)$, which we used to study the thermodynamics properties of vibrational mean energy $U(\beta)$, vibrational entropy $S(\beta)$, vibrational mean free energy $F(\beta)$, and vibrational specific heat capacity $C(\beta)$. Besides, the effective Boltzmann factor is calculated by using superstatistics, and the results is compared with the case where the deformation parameter vanished. It is noted that the results, in the special case of the vanished

deformation parameter, are in agreement with the ordinary statistics. Finally, this study has many applications in different areas of physics, and chemistry such as atomic physics, molecular physics and chemistry amongst others.

1. S. Dong, G. H. Sun, B. J. Falaye and S. H. Dong, Semi-exact solutions to position-dependent mass Schrödinger problem with a class of hyperbolic potential *V0tanh(ax)*. *Eur. Phys. J. Plus* **131** (2016) 176. https://doi.org/10.1140/epjp/i2016-16176-5
2. A. N. Ikot *et al.*, Superstatistics of Schrödinger equation with pseudo-harmonic potential in external magnetic and Aharanov-Bohm fields, *Heliyon* **6** (2020) e03738. https://doi.org/10.1016/j.heliyon.2020.e03738
3. S. Dong, G. H. Sun, and S. H. Dong, Arbitrary l-Wave Solutions of the Schrödinger Equation For The Screen Coulomb Potential, *Int. J. Mod Phys E*. **22** (2013) 1350036. https://doi.org/10.1142/S0218301313500365
4. A.N. Ikot *et al.,* Bound state solutions of the Schrödinger equation with energy dependent molecular Kratzer potential via asymptotic iteration method, *Eclet. Quim. J*. **45** (2020) 65. https://doi.org/10.26850/1678-4618eqj.v45.1.p65-76
5. H. Louis *et al.*, Solutions to the Dirac Equation for Manning-Rosen Plus Shifted Deng-Fan Potential and Coulomb-Like Tensor Interaction Using Nikiforov-Uvarov Method, *Intl. J. Chem.* **10** (2018) 99. https://doi.org/10.5539/ijc.v10n3p99
6. C.O. Edet, U.S. Okorie, A.T. Ngiangia and A.N. Ikot, Bound state solutions of the Schrödinger equation for the modified Kratzer potential plus screened Coulomb potential, *Ind. J. Phys.* **94** (2019) 425. https://doi.org/10.1007/s12648-019-01467-x
7. C. O. Edet, K. O. Okorie, H. Louis and N. A. Nzeata-Ibe, Any l-state solutions of the Schrödinger equation interacting with Hellmann-Kratzer potential model, *Indian J Phys* **94** (2020) 243. https://doi.org/10.1007/s12648-019-01477-9
8. C. S. Jia, P. Guo and X. L. Peng, Exact solution of the Dirac-Eckart problem with spin and pseudospin symmetry *J. Phys. A: Math. Gen*. **39** (2006) 7737. https://doi.org/10.1088/0305-4470/39/24/010
9. A. N. Ikot, S. Zarrinkamar, B. H. Yazarloo, and H. Hassanabadi, Relativistic symmetries of Deng-Fan and Eckart potentials with Coulomb-like and Yukawa-like tensor interactions. *Chin. Phys. B* **23** (2014) 100306. https://doi.org/10.1088/1674-1056/23/10/100306
10. B. J. Falaye, Any ℓ-state solutions of the Eckart potential via asymptotic iteration method. *Centr. Eur. J. Phys.* **10** (2012) 960. urlhttps://doi.org/10.2478/s11534-012-0047-6
11. H. Louis *et al.*, ℓ-state Solutions of the Relativistic and Non-Relativistic Wave Equations for Modified Hylleraas-Hulthen Potential Using the Nikiforov-Uvarov Quantum Formalism, *Oriental J. Phys. Sci.* **3** (2018) 1. http://www.orientjphysicalsciences.org/
12. W. A. Yahya, B. J. Falaye, O. J. Oluwadare and K. J. Oyewumi, Solutions of The Dirac Equation With The Shifted Deng-Fan Potential Including Yukawa-Like Tensor Interaction, *Intl. J. of Mod. Phys E* **22** (2013) 1350062. https://doi.org/10.1142/S0218301313500626
13. K. J. Oyewumi, B. J. Falaye, C. A. Onate, O. J. Oluwadare and W. A. Yahya, Thermodynamic properties and the approximate solutions of the Schrödingerequation with the shifted Deng-Fan potential model, *Mol. Phys*, **112** (2014) 127. https://doi.org/10.1080/00268976.2013.804960
14. H. Boukabcha, M. Hachama and A. Diaf, Ro-vibrational energies of the shifted Deng-Fan oscillator potential with Feynman path integral formalism. *Appl. Math. Comput*. **321** (2018) 12. https://doi.org/10.1016/j.amc.2017.10.044
15. R. Khordad and B. Mirhosseini, Application of Tietz potential to study optical properties of spherical quantum dots. *Pramana J. Phys*. **85** (2015) 723. https://doi.org/10.1007/s12043-014-0906-3
16. H. Nikoofard, E. Maghsoodi, S. Zarrinkamar, M. Farhadi, and H. Hassanabadi, The nonrelativistic molecular Tietz potential, *Turk J Phys* **37** (2013) 74. https://doi.org/10.3906/fiz-1207-1
17. G. J. Rampho, A. N. Ikot, C. O. Edet, and U. S. Okorie, Energy spectra and thermal properties of diatomic molecules in the presence of magnetic and AB fields with improved Kratzer potential, *Mol. Phys*, (2020) https://doi.org/10.1080/00268976.2020.1821922
18. C. O. Edet, P. O. Okoi, A. S. Yusuf, P. O. Ushie and P. O. Amadi, Bound state solutions of the generalized shifted Hulthe'n potential, *Indian J. Phys*. (2019) https://doi.org/10.1007/s12648-019-01650-0
19. R. L. Greene, C. Aldrich, Variational wave functions for a screened Coulomb potential, *Phys. Rev. A* **14** (1976) 2363. https://doi.org/10.1103/PhysRevA.14.2363
20. A. N. Ikot, C. O. Edet, P. O. Amadi, U. S. Okorie, G. J. Rampho, and H. Y. Abdullah, Thermodynamic properties of Aharanov-Bohm (AB) and magnetic fields with screened Kratzer potential, *Eur. Phys. J. D* **74** (2020) 159, https://doi.org/10.1140/epjd/e2020-10084-9
21. H. Fakhri and J. Sadeghi, Supersymmetry Approaches to The Bound States of The Generalized Woods-Saxon Potential. *Mod Phys Lett A*, **19** (2004) 615. https://doi.org/10.1142/S0217732304013313
22. C. N. Isonguyo, I. B. Okon, A. N. Ikot, and H. Hassanabadi, Solution of Klein Gordon Equation for Some Diatomic Molecules with New Generalized Morse-like Potential Using SUSYQM, *Bull. Kor. Chem. Soc*. **35** (2014) 3443. https://doi.org/10.5012/bkcs.2014.35.12.3443
23. A. Arai, J. Math. Exactly solvable supersymmetric quantum mechanics, *Anal. Appl.,* **158** (1991) 63. https://doi.org/10.1016/0022-247X(91)90267-4

24. A. N. Ikot, B. H. Yazarloo, E. Maghsoodi, S. Zarrinkamar, and H. Hassanabadi, Effects of tensors coupling to Dirac equation with shifted Hulthen potential via SUSYQM, *J. Assoc. Arab Uni. Basic Appl. Sci.*, **18** (2015) 46. https://doi.org/10.1016/j.jaubas.2014.03.005

25. C. O. Edet, P. O. Okoi, and S. O. Chima, Analytic solutions of the Schrödinger equation with non-central generalized inverse quadratic Yukawa potential, *Rev. Bras. Ens. Fis.* **42** (2019) e20190083. https://doi.org/10.1590/1806-9126-RBEF-2019-0083

26. P. O. Okoi, C. O. Edet and T. O. Magu, Relativistic treatment of the Hellmann-generalized Morse potential, *Rev. Mex. Fis.* **66** (2020) 1, https://doi.org/10.31349/RevMexFis.66.1

27. C. O. Edet and P. O. Okoi, Any l-state solutions of the Schrödinger equation for q-deformed Hulthen plus generalized inverse quadratic Yukawa potential in arbitrary dimensions *Rev. Mex. Fis.* **65** (2019) 333. https://doi.org/10.31349/RevMexFis.65.333

28. B. J. Falaye, Arbitrary l-State Solutions of the Hyperbolical Potential by the Asymptotic Iteration Method, *Few-Body Syst.* **53** (2012) 557. https://doi.org/10.1007/s00601-012-0440-0

29. H. Çiftçi, R. L. Hall, and N. Saad, Asymptotic iteration method for eigenvalue problems, *J. Phys. A Math Gen.* **36** (2003) 11807. https://stacks.iop.org/JPhysA/36/11807

30. H. Çiftçi, R. L. Hall, and N. Saad, Perturbation theory in a framework of iteration methods, *Phys. Lett. A* **340** (2005) 388. https://doi.org/10.1016/j.physleta.2005.04.030

31. F. Chafa, A. Chouchaoui, M. Hachemane, and F. Z. Ighezou, The quasi-exactly solvable potentials method applied to the three-body problem. *Ann. Phys.* **322** (2007) 1034. https://doi.org/10.1016/j.aop.2006.07.007

32. A. N. Ikot, L. E. Akpabio and A. D. Antia, Path Integral of Time-Dependent Modified Caldirola-Kanai Oscillator. *Arab. J. Sci. Eng.* **37** (2012) 217. https://dx.doi.org/10.1007/s13369-011-0160-7

33. A. Diaf and A. Chouchaoui, l-states of the Manning-Rosen potential with an improved approximate scheme and Feynman path integral formalism. *Phys. Scr.* **84** (2011) 015004. https://doi.org/10.1088/0031-8949/84/01/015004

34. A. Khodja, F. Benamira, and L. Guechi, Path integral discussion of the improved Tietz potential. *J. Math. Phys.* **59** (2018) 042108. https://doi.org/10.1063/1.5022285

35. C. O. Edet, U. S. Okorie, G. Osobonye, A. N. Ikot, G. J. Rampho and R. Sever, Thermal properties of Deng-Fan-Eckart potential model using Poisson summation approach, *J. Math. Chem.* **58** (2020) 989. https://doi.org/10.1007/s10910-020-01107-4

36. U. S. Okorie, A. N. Ikot, C. O. Edet, I. O. Akpan, R. Sever and R. Rampho, Solutions of the Klein Gordon equation with generalized hyperbolic potential in D-dimensions, *J. Phys. Commun.* **3** (2019) 095015. https://doi.org/10.1088/2399-6528/ab42c6

37. B. J. Falaye, S. M. Ikhdair, and M. Hamzavi, Formula Method for Bound State Problems. *Few-Body Syst* **56** (2015) 63. https://doi.org/10.1007/s00601-014-0937-9

38. B. I. Ita, H. Louis, O. U. Akakuru, N. A. Nzeata-Ibe, A. I. Ikeuba, T. O. Magu, P. I. Amos and C. O. Edet, Approximate Solution to the SchrödingerEquation with Manning-Rosen plus a Class of Yukawa Potential via WKBJ Approximation Method, *Bulg. J. Phys.* **45** (2018) 323. https://www.bjp-bg.com/paper1.php?id=914

39. X. Y. Gu, S. H. Dong, and Z. Q. Ma, Energy spectrum for a modified Rosen-Morse potential solved by proper quantization rule and its thermodynamic properties. *J. Phys. A: Math. Theor*. **42** (2009) 035303. https://doi.org/10.1007/s10910-011-9931-3

40. S.M. Ikhdair and J. Abu-Hasna, Quantization rule solution to the Hulthén potential in arbitrary dimension with a new approximate scheme for the centrifugal term. *Phys. Scr.* **83** (2011) 025002. https://doi.org/10.1088/0031-8949/83/02/025002

41. B. J. Falaye, S. M. Ikhdair and M. Hamzavi, Shifted Tietz-Wei oscillator for simulating the atomic interaction in diatomic molecules. *J. Theor. Appl. Phys.* **9** (2015) 151. https://doi.org/10.1007/s40094-015-0173-9

42. S.H. Dong, D. Morales, and J. Garcia-Ravelo, Exact Quantization Rule and Its Applications to Physical Potentials. *Int. J. Mod. Phys. E*, **16** (2007) 189. https://doi.org/10.1142/S0218301307005661

43. W. C. Qiang and S. H. Dong, Proper quantization rule. *Europhys. Lett*. **89** (2010) 10003. https://doi.org/10.1209/0295-5075/89/10003

44. B.J. Falaye, S.M. Ikhdair, and M. Hamzavi, Spectroscopic study of some diatomic molecules via the proper quantization rule. *J Math Chem* **53** (2015) 1325. https://doi.org/10.1007/s10910-015-0491-9

45. S. H. Dong and M. Cruz-Irisson, Energy spectrum for a modified Rosen-Morse potential solved by proper quantization rule and its thermodynamic properties. *J. Math. Chem.* **50** (2012) 881. https://doi.org/10.1007/s10910-011-9931-3

46. O. J. Oluwadare, and K. J. Oyewumi, Energy spectra and the expectation values of diatomic molecules confined by the shifted Deng-Fan potential. *Eur. Phys. J. Plus* **133** (2018) 422. https://doi.org/10.1140/epjp/i2018-12210-0

47. X. Y. Gu and S. H. Dong, Energy spectrum of the Manning-Rosen potential including centrifugal term solved by exact and proper quantization rules. *J. Math. Chem*. **49** (2011) 2053. https://doi.org/10.1007/s10910-011-9877-5

48. F. A. Serrano, X. Y. Gu, and S. H. Dong, Qiang-Dong proper quantization rule and its applications to exactly solvable quantum systems. *J. Math. Phys*. **51** (2010) 082103. https://doi.org/10.1063/1.3466802

49. M. Hamzavi and A. A. Rajabi, Solution of Dirac equation with Killingbeck potential by using wave function ansatz method under spin symmetry limit. *Commun. Theor. Phys.* **55** (2011) 35. https://doi.org/10.1088/0253-6102/55/1/07

50. G. Pöschl and E. Teller, Bemerkungen zur Quantenmechanik des anharmonischen Oszillators. *Z. Phys.* **83** (1933) 143. https://doi.org/10.1007/BF01331132

51. X. W. Liu, G. F. Wei, X. W. Cao, and H. G. Bai, Spin Symmetry for Dirac Equation with the Trigonometric Pöschl-Teller Potential, *Int. J. Theor. Phys.* **49** (2010) 343. https://doi.org/10.1007/s10773-009-0207-7

52. B. J. Falaye and S. M. Ikhdair, Relativistic symmetries with the trigonometric Pöschl-Teller potential plus Coulomb-like tensor interaction, *Chin. Phys. B*, **22** (2013) 060305, https://doi.org/10.1088/1674-1056/22/6/060305

53. M. Hamzavi, A. A. Rajabi, and M. Amirfakhrian, Approximate Solution of the Spin-0 Particle Subject to the Trigonometric Pöschl-Teller Potential with Centrifugal Barrier. *Z. Naturforsch.* **68a** (2013) 524. https://doi.org/10.5560/ZNA.2013-0030

54. N. Candemir Spin and Pseudospin, Symmetries in Relativistic Trigonometric Pöschl-Teller Potential with Centrifugal Barrier. *Intl J. Mod Phys E* **21** (2012) 1250097. https://doi.org/10.1142/S0218301312500978

55. M. Hamzavi and A. A. Rajabi, Spin and Pseudospin Symmetries with Trigonometric Pöschl-Teller Potential including Tensor Coupling. *Adv. High Energy Phys* **2013** (2013) 196986, http://dx.doi.org/10.1155/2013/196986

56. M. Hamzavi and A.A. Rajabi, Exact S-wave solution of the trigonometric Pöschl-Teller potential, *Int. J. Quant. Chem.* **112** (2012) 1592. https://doi.org/10.1002/qua.23166

57. M. Hamzavi and S. M. Ikhdair, Approximate l-state solution of the trigonometric Pöschl-Teller potential. *Mol. Phys* **110** (2012) 3031. https://doi.org/10.1080/00268976.2012.695029

58. A. N. Ikot, E. O. Chukwuocha, M. C. Onyeaju, C. A. Onate, B. I. Ita. and M. E. Udoh, Thermodynamics properties of diatomic molecules with general molecular potential, Pramana. *J. Phys.* **90** (2018) 22. https://doi.org/10.1007/s12043-017-1510-0

59. U. S. Okorie, C. O. Edet, A. N. Ikot, G. J. Rampho and R. Sever, Thermodynamic functions for diatomic molecules with modified Kratzer plus screened Coulomb potential. *Ind. J. Phys.* (2020). https://doi.org/10.1007/s12648-019-01670-w

60. A. N. Ikot *et al*., *Exact and Poisson summation thermodynamic properties for diatomic molecules with shifted Tietz potential*, (2019). *Indian J. Phys*, https://doi.org/10.1007/s12648-019-01375-0

61. G. Herzberg, *Molecular spectra and molecular structure II*, Infared and Raman spectra of polyatomic molecules (Van Nostrand, New York, 1945).

62. A. N. Ikot, B. C. Lutfuoglu, M. I. Ngwueke, M. E. Udoh, S. Zare and H. Hassanabadi, Klein-Gordon equation particles in exponential-type molecule potentials and their thermodynamic properties in D dimensions, *Eur. Phys. J. Plus* **131** (2016) 419. https://doi.org/10.1140/epjp/i2016-16419-5

63. H. J. Korsch, A new semiclassical expansion of the thermodynamic partition function, *J. Phys. A: Math. Gen.* **12** (1979) 1521. https://doi.org/10.1088/0305-4470/12/9/019

64. G. Wilk and Z. Wlodarczyk, Interpretation of the Nonextensivity Parameter q in Some Applications of Tsallis Statistics and Lévy Distributions, *Phys. Rev. Lett.* **84** (2000) 2770. https://doi.org/10.1103/PhysRevLett.84.2770

65. H. Touchette and C. Beck, Asymptotics of superstatistics *Phys. Rev. E* **71** (2005) 016131. https://doi.org/10.1103/PhysRevE.71.016131

66. C. Beck and E. G. D. Cohen, Superstatistics, *Physica A* **322** (2003) 267. https://doi.org/10.1016/S0378-4371(03)00019-0

67. D. Bonatsos and C. Daskaloyannis, Quantum Groups in Nuclear Spectra and in Metal Clusters, *Prog. Part. Nucl. Phys.* **43** (1999) 537. http://dx.doi.org/10.12681/hnps.2209

68. H. Hassanabadi, S. Sargolzaeipor, and W. S.Chung, Superstatistics properties of -deformed Morse potential in one dimension, *Physica A*, **508** (2018) 740. https://doi.org/10.1016/j.physa.2018.05.125

69. S. Sargolzaeipor, H. Hassanabadi and A. Boumali, Morse potential of the q-deformed in the Duffin-Kemmer-Petiau equation, *Int. J. Geom. Methods Mod. Phys.* **14** (2017) 1750112. https://doi.org/10.1142/S0219887817501122

70. S. Sargolzaeipor, H. Hassanabadi and W. S. Chung, The q-deformed Dirac oscillator in the presence of a magnetic field in (1+2)-dimensions in Noncommutative phase space, *J. Korean Phys. Soc.* **70** (2017) 557. https://doi.org/10.3938/jkps.70.557

71. C. Beck, Dynamical Foundations of Nonextensive Statistical Mechanics, *Phys. Rev. Lett.* **87** (2001) 180601. https://doi.org/10.1103/PhysRevLett.87.180601

72. C. Tsallis and A. M. C. Souza, Constructing a statistical mechanics for Beck-Cohen superstatistics, *Phys. Rev. E* **67** (2003) 026106. https://doi.org/10.1103/PhysRevE.67.026106

73. C. Beck, Superstatistics: theory and applications. *Continuum Mech. Thermodyn.* **16** (2004) 293. https://doi.org/10.1007/s00161-003-0145-1

74. C. Tsallis, Possible generalization of Boltzmann-Gibbs statistics, *J. Stat. Phys.* **52** (1988) 479. https://doi.org/10.1007/BF01016429

75. S. Sargolzaeipor, H. Hassanabadi and W. S. Chung, Superstatistics of two electrons quantum dot, *Mod. Phys Lett A.* **34** (2018) 1950023. https://doi.org/10.1142/S0217732319500238

76. B. J. Falaye, Corrigendum: Energy spectrum for trigonometric Pöschl-Teller potential solved by the asymptotic iteration method, *Can. J. Phys.* **91** (2013) 365. https://dx.doi.org/10.1139/cjp-2013-0011